Dynamic immunological changes in tumor microenvironment during treatment of cervical cancer and an analysis of immunological differences related to prognosis

Kyunglim Lee

The Graduate School
Yonsei University
Department of Medicine

Dynamic immunological changes in tumor microenvironment during treatment of cervical cancer and an analysis of immunological differences related to prognosis

A Master's Thesis Submitted
to the Department of Medicine
and the Graduate School of Yonsei University
in partial fulfillment of the
requirements for the degree of
Master of Medical Science

Kyunglim Lee

December 2024

This certifies that the Master's Thesis of Kyunglim Lee is approved

Thesis Supervisor Jung Yun Lee

Thesis Committee Member Eunhyang Park

Thesis Committee Member Junsik Park

The Graduate School
Yonsei University
December 2024

TABLE OF CONTENTS

LIST OF FIGURES

LIST OF TABLES

ABSTRACT

Dynamic immunological changes in tumor microenvironment during treatment of cervical cancer and an analysis of immunological differences related to prognosis

Globally, cervical cancer is the fourth most common cancer in women. In locally advanced cervical cancer (LACC), cisplatin-based concurrent chemoradiotherapy (CCRT) is established as the standard treatment. However, the 5-year disease-free survival rate is approximately 58%, indicating the need for further research to improve survival outcomes.

Dynamic changes in tumor-infiltrating lymphocytes (TILs) have been reported after CCRT in various cancers. Therefore, ongoing research on TILs may offer new insights for combining standard cancer treatments with immunotherapy. This study aimed to analyze dynamic changes in TILs during CCRT in patients with LACC and obtain an in-depth understanding of the CCRT-induced changes in the tumor microenvironment.

Forty-one patients with cervical cancer were enrolled between March 2020 and July 2023 at the Yonsei Cancer Center, Seoul, Republic of Korea. TILs were isolated from fresh tumor tissues (treatment naïve samples, n = 39; on-CCRT samples, n = 9). The immunologic characteristics of TILs were analyzed by multi-color flow cytometry using fluorescence-activated cell sorting (FACS). Peripheral blood mononuclear cells were isolated for the 21 patients with available blood samples, and subjected to flow cytometry concomitantly.

The median age of patients was 51 years (range 27–85). Thirty-six patients (87.8%) had LACC and IIIC was the most common disease stage in our cohort (n = 19, 46.3%). Human papillomavirus (HPV) infection was confirmed in all but two patients.

Significantly fewer $CD45^+$ hematopoietic cells were noted during CCRT. Overall, TILs were more exhausted than PBMCs. In CD8 TILs, co-inhibitory receptors including PD-1, TIM-3, LAG-3, and TIGIT showed no significant changes during CCRT. Granzyme B expression was significantly increased among CD8 TILs, while $TCF\text{-}1^+PD\text{-}1^+$ CD8 TILs (stem-like CD8 T cells) were significantly decreased during CCRT. The proliferation marker Ki-67 was decreased in regulatory T cells. Additionally, $L1CAM^+$ tumor cells were decreased after CCRT.

On stratifying patients according to post-CCRT progression-free survival (PFS), there was no

difference in CD8 TILs among naive samples between the long PFS (over 18 months) and short PFS groups. When comparing CD8 TILs, no significant differences were observed in PD-1^{+} cells based on prognosis. However, analysis of TIM-3 and LAG-3 expression showed a trend toward decreased expression in the good prognosis group and increased expression in the poor prognosis group during treatment. Since TIM-3 and LAG-3 are expressed in terminally exhausted T cells, reduction in these cells may be associated with better clinical outcomes. In contrast, the poor prognosis group showed increased TIM-3 and LAG-3 expression post-treatment, suggesting a potential role for immunotherapy targeting these receptors.

The immune properties of TILs in cervical cancer appear to dynamically change during CCRT. Examining the CCRT-induced changes in the tumor microenvironment in cervical cancer and characterizing their association with prognosis may provide insights for developing new strategies for combining conventional treatments with immunotherapy.

Key words: Cervical cancer, CCRT, Peripheral blood mononuclear cells, Tumor-infiltrating lymphocytes, Tumor microenvironment

I. INTRODUCTION

1.1. Research background

1.1.1. Introduction to cervix cancer

In 2020, cervical cancer was the fourth most prevalent cancer among women worldwide, following breast, colorectal, and lung cancers. Human papillomavirus (HPV) vaccinations are being implemented globally to combat this disease, as HPV is the primary cause of cervical cancer. Additionally, PAP smear tests, a screening method for cervical cancer, are part of the national health screening program. Despite these protective methods, according to the “Korean Cancer Registration and Statistics Program Annual Report 2019,” cervical cancer remained a significant concern in Korea. It ranked fifth in prevalence among women, with 58,983 reported cases, and 10th in incidence, with 3,273 new cases diagnosed annually. The 5-year survival rate for cervical cancer varies significantly depending on the stage at diagnosis. According to the Centers for Disease Control and Prevention (CDC) statistics in the United States, the 5-year survival rate is favorable for localized cases, at 90.6%. However, the rate drops to 59.1% for cases with regional metastasis and sharply declines to 19.1% in cases with distant metastasis.

1.1.2. Introduction to standard treatment for locally advanced cervical cancer

Locally advanced cervical cancer (LACC) is defined from stages IB2 to IVA by International Federation of Gynecology and Obstetrics (FIGO) 2018 staging system. Stage IB2 is characterized by a tumor size exceeding 2 cm, while stage IVA indicates tumor invasion into adjacent pelvic organs, such as the bladder or rectum. According to a large-scale systemic review, most guidelines recommend CCRT for LACC. However, for earlier stages (IB2 to IIA2), radical hysterectomy is often suggested as an alternative. Therefore, CCRT is commonly administered for more advanced stages (IIB to IVA) in LACC. The standard treatment with CCRT involves weekly administration of cisplatin at 40 mg/m² along with external beam radiation therapy followed by vaginal brachytherapy. The 5-year disease-free survival rate after CCRT for cervical cancer is approximately 58%, and the overall survival rate is about 66%.

1.1.3. Introduction to peripheral blood mononuclear cells and tumor-infiltrating lymphocytes

Peripheral blood mononuclear cells (PBMCs) include monocytes, lymphocytes, including T cells, and dendritic cells. PBMCs serve as a valuable source for analyzing systemic immune responses in cancer patients.

In cancer patients, immune cells present in the blood migrate to the tumor tissue, where tumor-infiltrating lymphocytes Tumor-infiltrating lymphocytes (TILs) are formed. The presence of TILs reflects the dynamic interplay between the host immune system, tumor antigens, and the tumor microenvironment. As such, the TIL profile provides valuable insights into the local immune response to cancer.

Research is underway to analyze the characteristics of TILs and gain valuable information for assessing tumor progression and treatment prognosis. Numerous studies have established that a higher pre-treatment density of $CD8^+$ TILs in cervical cancer patients is associated with a better prognosis following radiation therapy or CCRT. A high proportion of activated cytotoxic T cells within the tumor typically correlates with better clinical outcomes, as these cells can direct kill cancer cells.

Comparing the immune profiles of PBMCs and TILs can provide insights into systemic versus local immune responses. Studies have demonstrated distinct alterations in PBMCs and TILs in cervical cancer patients. For instance, the tumor microenvironment contains higher levels of $CD8^+$ T cells and lower $CD4^+$ T cells than peripheral blood.

Chronic exposure to tumor antigens inevitably leads to exhaustion of TILs. This exhausted state is characterized by the upregulation of inhibitory receptors such as PD-1, LAG-3, CTLA-4, and CD39, accompanied by a decrease in the transcription factor TCF-1, and an increase in the exhaustion marker TOX.

In a previous study, CCRT treatment was found to induce a decrease in T cell counts in both the tumor and blood, alongside an increase in the presence of macrophages and neutrophils in the tumor tissue. Significant changes in immune cell composition were observed between pre-treatment and post-CCRT groups. Another study demonstrated a decrease in PD-1^+ $CD8^+$ T cells, PD-1^+ $CD4^+$ T cells, and PD-L1 expression in the peripheral blood samples after CCRT in cervical cancer patients. These findings demonstrate that CCRT treatment indeed induces immunological changes in not only blood but also tissue.

2. MATERIALS AND METHODS

2.1 Patients and tumor lymphocyte and PBMC isolation

A total of 41 patients with cervical cancer were enrolled between March 2020 to July 2023 at the Yonsei Cancer Center, Seoul, Republic of Korea. Among them, blood samples for peripheral blood analysis were obtained from 21 patients. Patient tissue samples were obtained through cervical punch biopsy or during surgery. The clinical characteristics of the study population are summarized in Table 1.

The patient cohort had a median age of 51 years (range 27–85). Of these, 36 patients (87.8%) had LACC, with stage IIIC disease being the most common (n = 19, 46.3%). Of the 36 patients with LACC, 13 received standard CCRT as the initial treatment. Among these, seven had paired samples available for analysis, both before and after treatment.

Tumor-infiltrating lymphocytes were isolated from tumor tissues within 24 hours of biopsy using the Gentle MACS C-Tube (Milteny Biotec, Germany). The isolation process involved the enzymatic breakdown of the tumor tissue into single cells using the 'Gentle MACS Dissociator'. The resulting cell suspension was filtered through a 70 μm strainer, washed twice with Dulbecco's Phosphate-Buffered Saline (DPBS), centrifuged, and aspirated to obtain the isolated TILs.

For the 21 patients with available blood samples, PBMC isolation was also performed. The blood samples were mixed with DPBS at approximately a 1:1 ratio and carefully layered over Ficoll, maintaining a 1:1:1 ratio. The sample was centrifuged for 20 minutes, and the PBMC layer was transferred to a tube using a pipette aid. The sample was then washed with PBS for 10 minutes, and the supernatant was removed by suction. After adding PBS again to create a suspension, cell counting was performed using a C-chip and trypan blue. Both the isolated TILs and PBMCs were cryopreserved using freezing media.

All patients voluntarily provided written informed consent for participation in the study. This study was conducted in accordance with the ethical principles enshrined in the Helsinki Declaration.

Table 1. Clinical characteristics of the study population

Variables	All patients (n = 41)	Patients with blood samples (n = 21)
Age (median, range)	51 (27–85)	51 (25–85)
Histological classification		
Squamous cell carcinoma	30 (73.2%)	12 (57.1%)
Adenocarcinoma	6 (14.6%)	6 (28.6%)
Adenosquamous cell carcinoma	3 (7.3%)	2 (9.5%)
Neuroendocrine carcinoma	1 (2.4%)	0 (0%)
Clear cell carcinoma	1 (2.4%)	1 (4.8%)
FIGO Stage		
IA, IB1, IB2, IB3	1 (2.4%), 2 (4.9%), 8 (19.5%), 2 (4.9%)	1 (4.8%), 2 (9.5%), 6 (28.6%), 2 (9.5%)
IIA, IIB	2 (4.9%), 0 (0%)	2 (9/5%), 0 (0%)
IIIA, IIIB, IIIC	1 (2.4%), 3 (7.3%) 19 (46.3%)	0 (0%), 0 (0%), 7 (33.3%)
IVA, IVB	1 (2.4%), 2 (4.9%)	1 (4.8%), 0 (0%)
HPV status		
16 or 18	24 (58.5%)	12 (57.1%)
Other type	11 (26.8%)	6 (28.6%)
Unknown	4 (9.8%)	1 (4.8%)
Negative	2 (4.9%)	2 (9.5%)

Table 2. Detailed clinical information of all patients

Patient number	Age	Stage	Histologic type	Initial SCC (ng/mL)	Initial CA 125 (U/mL) (non-SCC type)	HPV status	Timing of biopsy	Biopsy method
1*	79	IIIA	SCC	>70.0		58	naïve, after C3	Punch biopsy
2**	43	IIIC	SCC	0.7		16	naïve	Punch biopsy
3*	59	IIIC	SCC	51.4		16	naïve, after C1	Punch biopsy
4	60	IVB	Adenosquamous Carcinoma	11.3	98.6	18	naïve	Punch biopsy
5	51	IIIB	SCC	3		Unknown	naïve	Punch biopsy
6	51	IIIC	SCC	41.5		35	naïve	Punch biopsy
7*	31	IIIC	SCC	20.3		16,18	naïve, after C2W1	Punch biopsy
8*	64	IIIC	SCC	3.1		16	after C1, after C4	Punch biopsy
9**	46	1B3	Adenocarcinoma	3.3	14.8	18	naïve	Operation
10	52	IIIC	SCC	55.9		16	naïve	Punch biopsy
11	36	IB2	Small cell neuroendocrine Carcinoma	0.9	15.2	18	naïve	Operation
12**	62	IA1	Clear cell carcinoma	0.9	11.6	Negative	naïve	Operation
13*	66	IIIC	SCC	25.7		68	naïve, after C1	Punch biopsy

14**	44	IIA	SCC	4.3		other type	naïve	Operation
15	55	IIIC	SCC	16		68	naïve	Punch biopsy
16**	57	1B2	SCC	0.4		Negative	naïve	Operation
17*	50	IIIB	SCC	39.1		Unknown	naïve, after C4	Punch biopsy
18	44	IIIC	SCC	9.4		16	naïve	Punch biopsy, Operation
19*	49	IIIC	SCC	16.7		Unknown	naïve, after C3	Punch biopsy
20*	65	IIIC	SCC	6.5		other type	naïve, after C3	Punch biopsy
21	27	1B2	SCC	1.5		16	naïve	Punch biopsy, Operation
22*	51	IIIB	SCC	5.9		16	after C4, after C5	Punch biopsy
23	43	IVB	SCC	11		16	naïve	Punch biopsy
24	40	IIIC	SCC	>70.0		16	naïve	Punch biopsy
25**	76	IB1	SCC	1		16	naïve	Operation
26**	56	IB2	Adenocarcinoma	1.2	14.8	18	naïve	Operation
27**	59	IB2	SCC	4.1		35,51	naïve	Operation
28**	54	IVA	Adenocarcinoma	0.6	19.8	other type	naïve	Operation

29**	51	IIIC1	Adenosquamous Carcinoma	0.9	14.1	16,52,53,56	naïve	Operation
30**	50	IB2	SCC	1.3		51	naïve	Operation
31**	85	IIA1	Adenocarcinoma	1	11.7	16	naïve	Operation
32**	82	IIIC1	SCC	16.7 (postop)		Unknown	naïve	Operation
33**	25	IB3	SCC	1.5		other type	naïve	Operation
34**	47	1B1	SCC	1.1		52	naïve	Operation
35**	66	IIIC	SCC	3		16	naïve	Operation
36**	52	IIIC	Adenocarcinoma	1.9	36	18,52	naïve	Operation
37**	34	1B2	SCC	3.7		16	naïve	Operation
38**	53	1B2	Adenocarcinoma		17.8	16	naïve	Operation
39**	40	IIIC	Adenosquamous Carcinoma	0.8	4.4	18	naïve	Operation
40	43	IIIC	SCC	44.8		18	naïve	Punch biopsy
41**	45	IIIC	SCC	13.5		16	naïve	Operation

* Patients with specimens associated with CCRT

** Patients for whom both blood and tumor samples were analyzed

SCC, squamous cell carcinoma; C, cycle; W, week

2.2 Sample preparation–Cell thawing

The cryotube was thawed in 37℃ water for 5 minutes. DNase I ($50X$) was added to the cryotube at a volume of 40 μL, followed by the addition of 1 mL of RPMI. After 5 minutes, the cells were transferred to a conical tube. The cryotube was then rinsed with 2 mL of PBS to ensure that all cells were recovered. Finally, the thawed cells were stained for flow cytometry analysis.

2.3. Immunostaining and flowcytometry

The cells were divided into two groups. Group 1 underwent FACS analysis immediately after cell surface staining. Group 2 underwent both cell surface staining and intracellular staining.

FACS analysis was performed using CD45, CD3, CD8, CD4, CD25, FoxP3, anti-PD1, anti-TIM-3, anti-LAG-3, TIGIT, CD39, CD103, Granzyme B, Ki-67, TOX, TCF-1, CTLA-4, 4-1BB, and CCR8.

Cell surface staining was a common step for both groups. For group 2, intracellular staining was performed sequentially after cell surface staining.

The prepared cells were washed with PBS and surface stained at 4°C in dark for 30 minutes using the following antibodies: BV 421-labeled anti-CD226, BV-421 labeled anti-PD-1, BV 510-labeled anti-CD3, BV 605-labeled anti-PD-1, BV 605-labeled anti-CD45RA, BV 605-labeled anti-CD25, BV 711-labeled anti-TIM-3, BV 711-labeled anti-CD127, BV711-labeled anti-CD45, BV 786-labeled anti-CD4, BV-labeled anti-CD16, BB515-labeled anti-CD39, BB515-labeled anti-CD73, PerCP-eFluor-labeled anti-CD103, PerCP-eFluor 710-labeled anti-4-1BB, PE-labeled anti CD-94, PE-labeled anti-L1CAM, PE-Cy7-labeled anti-TIGIT, PE-Cy7-labeled anti-PD-L1, APC-labeled anti-CCR8, APC-labeled anti-LAG3, APC-labeled anti-EpCAM, Af700-labeled anti-CD8. Af405-labeled antiA2R, and SB600-labeled anti-CD56. The classification of live and dead cells was performed together using staining with APC-H7-labeled live/dead™ fixable near-IR stain.

Following cell surface staining, the cells are washed with PBS at 4°C for 10 minutes. Subsequently, intracellular staining was performed, which involved fixation and permeabilization steps. Intracellular staining was performed for 30 minutes at 4°C in the dark using the following antibodies: FITC-labeled anti-Granzyme B, PerCP-eFlour labeled anti-Ki-67, PE-labeled anti-TOX, PE-Cy7-labeled anti-FoxP3, PE-labeled anti-FoxP3, APC-labeled anti-TCF-1, and PE-Cy7-labeled anti-CTLA-4.

Table 3. Resources used in the experiments

Reagent and Experimental materials	Company
Chemicals	
DPBS	Welgene
RPMI 10%	Cytiva
Transription factor staining buffer set	eBioscience
DNase I ($50X$)	Worthington-Biochem
Live/dead^{TM} fixable near-IR stain	Invitrogen
Others	
FACSLyric	BD Bioscience
FACS tube	FALCON

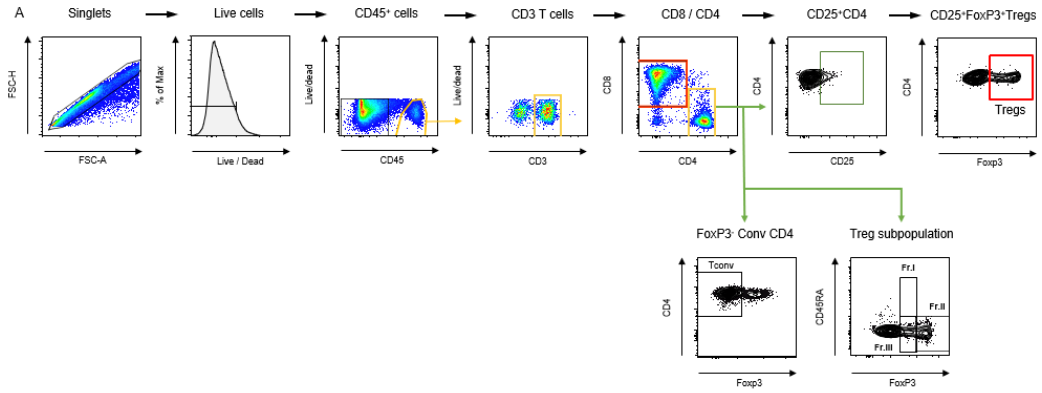

Figure 1. Gating strategies for flow cytometry

A) Gating strategies for flow cytometry analysis of immune cells.

First, single cells were sorted, and live cells were selected. Among them, $CD45^+$ cells, expressed in all nucleated hematopoietic cells, were further sorted. Then, CD3, a marker for T lymphocytes involved in immune activation and signaling, was identified. $CD3^+$ cells include $CD4^+$ T cells and $CD8^+$ T cells. Regulatory T cells (Tregs) were identified by co-expression of CD25 and Foxp3 markers, and further categorized into three subpopulations. Tumor cells were identified by selecting CD45-negative cells with positive expression of the epithelial cell marker EpCAM.

2.4 Statistical Analysis

The stained cells were analyzed on a FACSLyric flow cytometer (BD, Biosciences). The data were further analyzed using FlowJo software (Tree Star, OR, USA). Statistical analysis was conducted using Prism software version 6 (GraphPad Software, San Diego, CA). A significance level of $P \leq 0.05$ was considered statistically significant.

3. RESULTS

3.1. Characterization of tumor microenvironment of cervical cancer by analyzing PBMCs and TILs before treatment

CD8 T cells, conventional CD4 T cells, and regulatory T cells were significantly more abundant in TILs compared to PBMCs. This suggests that T cells had migrated from the peripheral blood into the tumor microenvironment. Among TILs, resting Tregs were significantly decreased compared to that among PBMCs, indicating a reduction in quiescent, antigen-unstimulated Tregs within the tumor microenvironment. Conversely, effector Treg cells were rarely detected in PBMCs but were significantly increased in TILs. Similarly, non-Treg cells exhibited some expression in PBMCs, but a significant increase was observed in TILs.

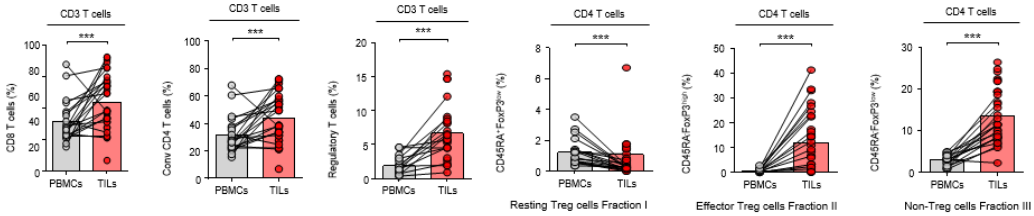

Figure 2. T cell composition of PBMCs and TILs before treatment

CD8 T cells, conventional CD4 T cells, and regulatory T cells (Tregs) are significantly more abundant in TILs compared to PBMCs. Further classification of Tregs into three subpopulations reveals a decrease in resting Tregs, which represent quiescent cells not subjected to antigenic stimulation, in TILs. In contrast, the other Treg subpopulations exhibit increased frequencies in TILs. The statistical analysis was performed using the independent samples *t*-test or Mann–Whitney U-test. ***P < 0.001

3.1.1. Comparative analysis of CD8 T cells in pre-treatment PBMCs and TILs

CD8 T cells in TILs exhibited distinct characteristics compared to those in PBMCs. Specifically, the frequencies of PD-1^{+} cells, TIM-3^{+} cells, LAG-3^{+} cells, and TIGIT^{+} cells were significantly increased in TILs, indicating a higher proportion of dysfunctional T cells in the tumor microenvironment.

Furthermore, CD8 T cells expressing CD39, either alone or in combination with CD103, were significantly more abundant in TILs than PBMCs. CD39 contributes to immunosuppression by generating adenosine, a potent immunosuppressive molecule, in conjunction with CD73. CD103 facilitates immune cell adhesion and interaction with epithelial cells through its binding to E-cadherin.

Additionally, TOX, a marker of T cell exhaustion, was severely elevated in TILs, indicating a high degree of exhaustion. In contrast, markers of proliferation, Granzyme B and Ki-67, were significantly increased in TILs. TCF-1^{+} cells (stem-like cells), critical for T cell development and memory formation, were decreased in TILs. Collectively, these findings indicate that CD8 T cells exhibit a unique phenotype characterized by increased proliferation and exhaustion compared to PBMCs

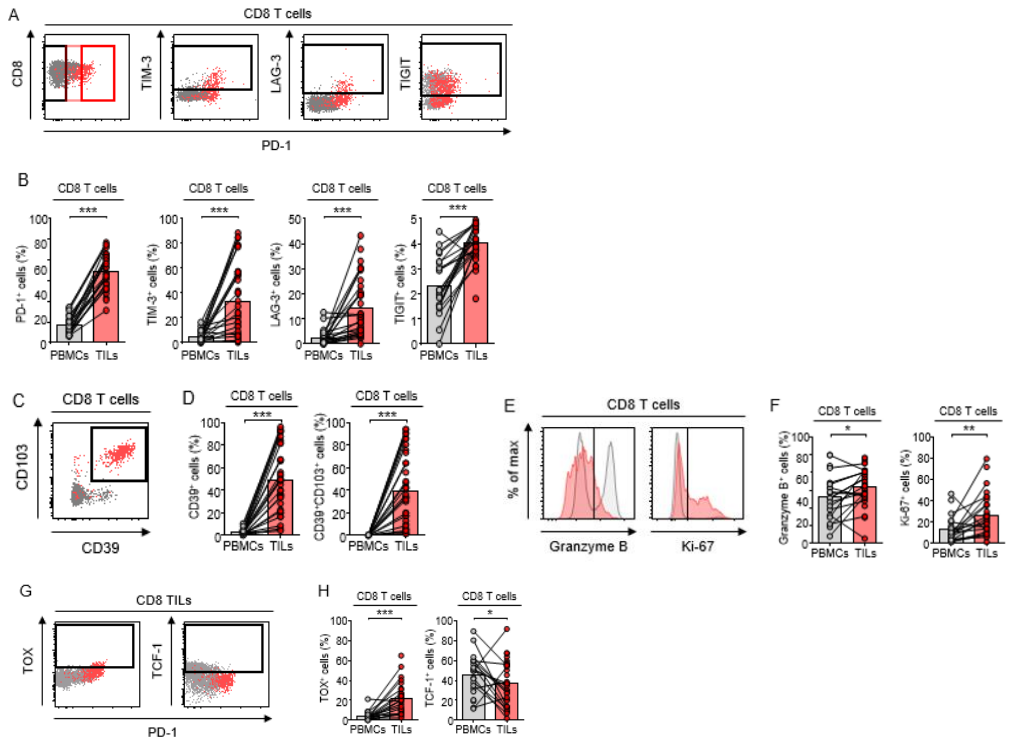

Figure 3. Comparative analysis of CD8 T cells in PBMCs and TILs

TILs are represented by red sections, while PBMCs are represented by black sections.

A) PD-1 expression in CD8 T cells is elevated in TILs (red) compared to PBMCs (black).

B) The frequencies of PD-1$^+$ cells, TIM-3$^+$ cells, LAG-3$^+$ cells, and TIGIT$^+$ cells are increased in TILs.

C, D) CD39$^+$ CD8 T cells and CD39$^+$CD103$^+$ double-positive CD8 T cells are enriched in TILs compared to PBMCs.

E, F) Granzyme B and Ki-67 expression are significantly higher in TILs compared to PBMCs.

G, H) In TILs, TOX levels were increased, while TCF-1 levels were decreased compared to PBMCs.

The independent samples *t*-test or Mann-Whitney U-test test was used for statistical analysis.

* $P < 0.05$; ** $P < 0.01$; *** $P < 0.001$.

3.1.2. Comparative analysis of conventional CD4 T cells in pre-treatment PBMCs and TILs

The expressions of PD-1, CTLA-4, and 4-1BB were significantly increased on conventional CD4 T cells in TILs compared to PBMCs. CTLA-4 is an immune checkpoint protein that plays crucial roles in inhibiting immune responses and preventing autoimmunity like PD-1. 4-1BB is a co-stimulatory molecule that enhances T-cell responses.

The frequencies of $CCR8^+$ and $CD39^+$ CD4 T cells were increased in TILs compared to PBMCs. CCR8 plays a major role in the immune response, including the trafficking and function of Tregs and Th2 cells.

In the analysis of Granzyme B and Ki-67 expression on CD 4 T cells, only Ki-67 showed a significant increase in TILs compared to PBMCs. TOX cells were increased in TILs, while TCF-1 cells were decreased, compared to PBMCs. These results indicate that TILs exist in a more exhausted state and have diminished T cell memory function compared to PBMCs. Consistent with the analysis of CD8 T cells, these findings suggest that conventional CD4 T cells also exhibit more proliferative and exhausted characteristics in TILs compared to PBMCs.

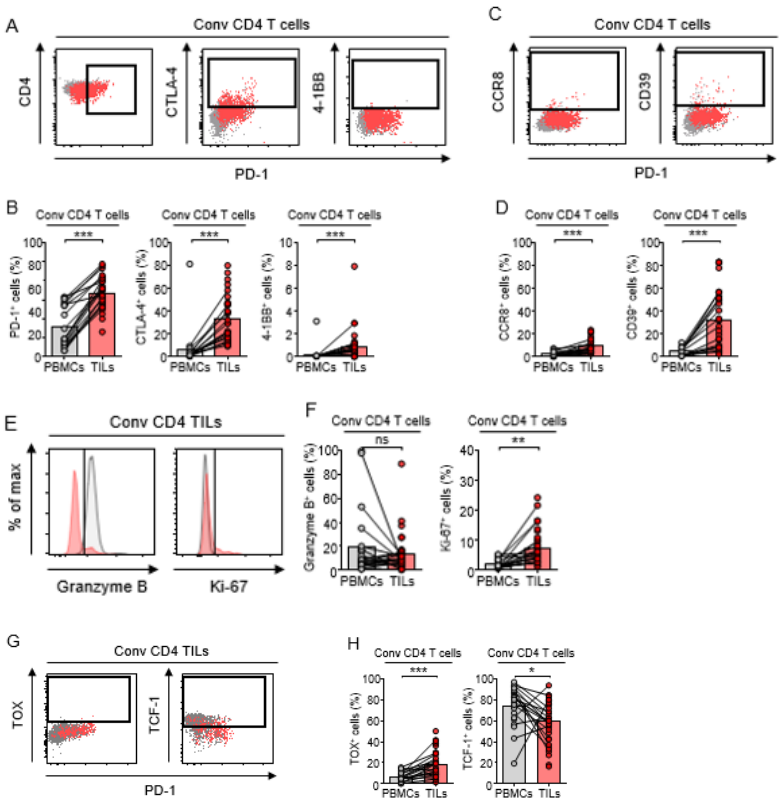

Figure 4. Comparative analysis of conventional CD4 T cells in PBMCs and TILs

A, B) Expressions of PD-1, CTLA-4, and 4-1BB are elevated on conventional CD 4 T cells in TILs compared to PBMCs.

C, D) Frequencies of CCR 8^{+} and CD 39^{+} conventional CD4 T cells are increased in TILs compared to PBMCs.

E, F) Analysis of Granzyme B and Ki-67 on conventional CD 4 T cells shows that only Ki-67 is significantly increased in TILs compared to PBMCs.

G, H) TOX^{+} cells are increased, whereas TCF-1^{+} cells are decreased in conventional CD4 T cells from TILs.

The statistical analysis was performed using the independent samples *t*-test or Mann-Whitney U-test. ns, non-significant;* $P < 0.05$; ** $P < 0.01$; ***$P < 0.001$

3.1.3. Comparative analysis of Treg cells in pre-treatment PBMCs and TILs

The expression of PD-1, CTLA-4, 4-1BB, CCR8, and CD 39 on Treg cells in TILs was significantly increased compared to PBMCs. While 4-1BB is known to stimulate effector T cells, its expression on Treg cells can modulate their suppressive function. CCR8 is involved in the migration of immune cells, particularly regulatory T cells (Tregs), to tumor sites. CCR8+ Tregs are believed to contribute to immune evasion by suppressing anti-tumor immune responses, allowing unchecked growth of cancer cells. Granzyme B expression on Tregs cells was decreased in TILs. Ki-67 expression remained unchanged. These findings suggest that tumor-infiltrating Treg cells were highly suppressive compared to PBMCs in patients with cervical cancer.

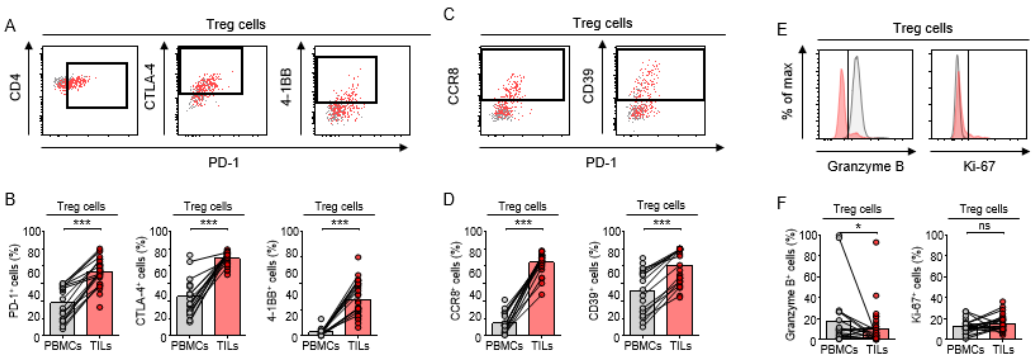

Figure 5. Comparative analysis of Treg cells in PBMCs and TILs

A, B) Expressions of PD-1, CTLA-4, and 4-1BB are increased on Treg cells in TILs.

C, D) Frequencies of $CCR8^{+}$ and $CD39^{+}$ Treg cells are increased in TILs.

E, F) Granzyme B expression is decreased, while Ki-67 expression shows no significant changes in Treg cells in TILs.

The independent samples *t*-test or Mann–Whitney U-test test was used for statistical analysis.

ns, nonsignificant;* $P < 0.05$; ***$P < 0.001$

3.2. Comparison of TILs between the pre-treatment group and on-treatment group

The clinical information of CCRT cases are provided in Table 4. All patients had squamous cell carcinoma with stage III disease. The CCRT regimen consisted of weekly cisplatin (40 mg/m^2 BSA) in six patients, while three patients received pembrolizumab (200 mg every 3 weeks) in combination with weekly cisplatin (40 mg/m²) as part of the MK 3475-A18 study. Out of the nine patients, paired samples (pre-treatment and on-treatment) were available for seven patients. The remaining two patients had two post-treatment samples collected at different time points following the initiation of CCRT.

Significantly fewer CD45$^+$ hematopoietic cells were noted during CCRT, indicating damage to these cells due to chemotherapy and radiation therapy. No significant changes in the distribution of CD3, CD8, conventional CD4, or Treg cells were observed before and after treatment.

Table 4. Clinical information of all patients with available specimens after the start of CCRT

	Pt	Age	Stage	Histologic type	Initial SCC (ng/mL)	HPV Status	Types of chemotherapy	Sample collection time	Progression	PFS (months)	PD-L1 status	Cervical mass size
Pair	1*	79	IIIA	SCC	>70.0	58	Cisplatin	naïve, after C3	yes	6.9	22C3 CPS50	6cm
Pair	3*	59	IIIC	SCC	51.4	16	MK 3475-A18	naïve, after C1	no	38.3	22C3 CPS5	5.7cm
pair	7*	31	IIIC	SCC	20.3	16,18	MK 3475-A18	naïve, after C2W1	yes	14.9	Negative	6cm
on-CCRT	8*	64	IIIC	SCC	3.1	16	Cisplatin	after C1, after C4	no	35.5	22C3 CPS10	3cm
pair	13*	66	IIIC	SCC	25.7	68	MK 3475-A18	naïve, after C1	yes	11.7	Unknown	6.6cm
pair	17*	50	IIIB	SCC	39.1	un-known	Cisplatin	naïve, after C4	no	34.0	22C3 CPS15	4.5cm
pair	19*	49	IIIC	SCC	16.7	un-known	Cisplatin	naïve, after C3	no	31.7	22C3 CPS3	6.5cm
pair	20*	65	IIIC	SCC	6.5	other type	Cisplatin	naïve, after C3	no	30.3	22C3 CPS5	5.7cm
on-CCRT	22*	51	IIIB	SCC	5.9	16	Cisplatin	after C4, after C5	yes	6.3	22C3 CPS15	6.8cm

*CCRT patients marked with an asterisk (*) in Table 2.

Pt : patients number

SCC: squamous cell carcinoma

MK 3475-A18: pembrolizumab 200 mg Q3weeks with weekly cisplatin 40 BSA

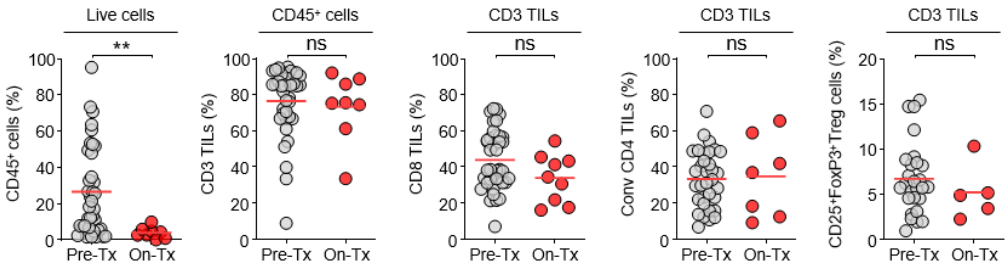

Figure 6. Immune cell compositional changes during CCRT

Graphs show the changes in CD45, CD3, CD8, conventional CD4, and Treg cells before and on-treatment.

The independent samples *t*-test or Mann–Whitney U-test test was used for statistical analysis.

ns, non-significant; **P < 0.01

3.2.1. Comparison of CD8 TILs

Co-inhibitory receptors such as PD-1, TIM-3, LAG-3, and TIGIT exhibited no significant changes during treatment. The expression of granzyme B was significantly increased among CD8 TILs.

TCF-1^{+}PD-1^{+}CD8 TILs (stem-like CD8 T cells) were significantly decreased during CCRT. No significant changes were observed in CD39, Ki-67, or TOX expression in CD8 TILs.

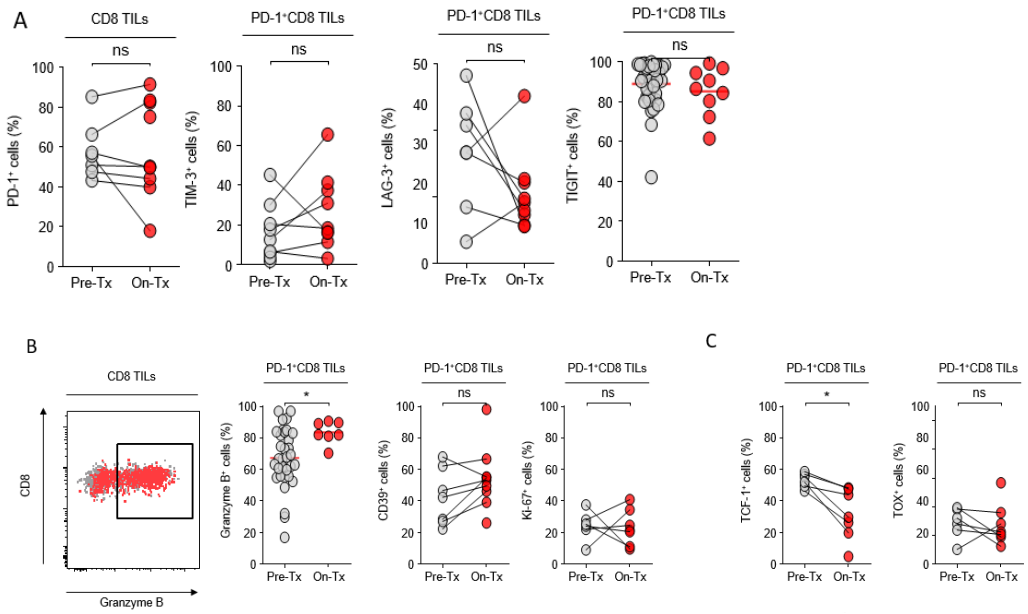

Figure 7. Differences in CD8 TILs between pre-treatment and on-treatment groups

A) PD-1, TIM-3, LAG-3, and TIGIT exhibit no significant changes during CCRT.

B) Changes in Granzyme B, CD39, and Ki-67 expression on CD8 TILs are observed during CCRT.

C) Changes in TCF-1 and TOX expression on CD8 TILs are observed during CCRT.

The independent samples *t*-test or Mann–Whitney U-test test was used for statistical analysis.

ns, non-significant; *P < 0.05

3.2.2. Comparison in TIL Tregs

CD39, CTLA-4, 4-1BB, CCR8, and Granzyme B expression on TIL Tregs showed no significant changes during CCRT. The expression of the proliferative marker Ki-67 on Tregs was decreased during CCRT.

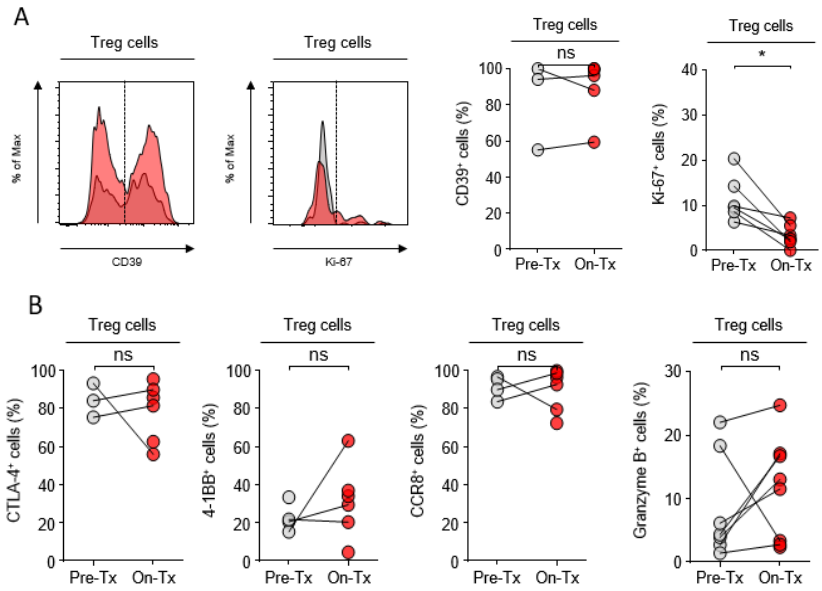

Figure 8. Difference in TIL Tregs between pre-treatment and on-treatment groups

A) Changes in CD39 and Ki-67 expression on TIL Tregs during CCRT.

B) Changes in CTLA-4, 4-1BB, CCR8, and Granzyme B expression on TIL Tregs during CCRT.

The independent samples *t*-test or Mann–Whitney U-test test was used for statistical analysis.

ns, nonsignificant; *P < 0.05

3.2.3. Comparison of tumor cells

Due to insufficient experimental samples, changes in PD-L1 expression in tumor cells before and after treatment could not be analyzed.

L1 Cell Adhesion Molecule (L1CAM) is a factor associated with poor prognosis, as it facilitates adhesion between vascular endothelium and tumor cells, thereby promoting metastasis. Notably, a statistically significant decrease in $L1CAM^{+}$ cells was observed in tumor cells.

VEGFR2 plays a key role in angiogenesis, promoting the formation of new blood vessels. Tumors require oxygen and nutrients for growth, and they meet these demands by forming new blood vessels through the VEGFR2 signaling pathway. A decrease in VEGFR2 expression often indicates a positive treatment response.

CD73 is a cell surface enzyme that converts AMP into adenosine, which has immunosuppressive effects. High CD73 expression promotes tumor growth, metastasis, and immune evasion, rendering treatment more challenging. Activation of adenosine A2A and A2B Receptors (A2a/bR) by adenosine suppresses the activity of immune cells, including T cells and NK cells.

A comparison of pre-CCRT and on-treatment samples revealed a decreasing trend in VEGFR2, CD73, and A2a/bR expression, although the changes were not statistically significant.

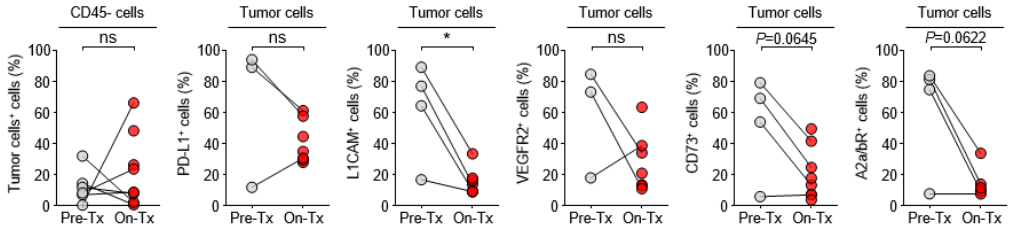

Figure 9. Changes in tumor cell markers following CCRT

Comparison of pre-treatment and on-treatment tumor cells revealed a statistically significant decrease only in L1CAM^{+} cells, while VEGFR2^{+}, CD73^{+}, and A2a/bR^{+} cells showed a trend toward decrease.

The independent samples *t*-test or Mann–Whitney U-test test was used for statistical analysis.

ns, nonsignificant; *P < 0.05

3.3. Comparison of TILs before and during treatment based on prognosis

Among the seven paired samples listed in Table 4, six had sufficient sample quantities for this analysis. We analyzed changes in TILs based on prognosis in these six patients (Table 5). These patients were categorized into two groups: those who experienced recurrence within 18 months (n = 3) and those who did not (n = 3).

When classified according to progression-free survival (PFS) after CCRT, no significant differences were observed in baseline characteristics between the long PFS (> 18 months) and short PFS groups. Higher levels of pre-treatment CD8 TILs are known to be associated with a better prognosis. However, in this analysis, pre-treatment CD8 TIL levels in the good prognosis group and poor prognosis group were similar, likely due to the small sample size.

T-cell populations were comparable between the two groups. When comparing CD8 TILs, no significant differences in PD-1+ cells were observed based on prognosis. However, analysis of TIM-3 and LAG-3 expression revealed a trend toward decreased expression in the good prognosis group and increased expression in the poor prognosis group.

Table 5. Patient list stratified by prognosis

Pt	Age	Stage	Histologic type	Initial SCC (ng/mL)	HPV Status	Types of chemotherapy	Sample collection time	Prog -ression	PFS (months)	PD-L1 status	Cervical mass size
Poor prognosis group											
Pair 1*	79	IIIA	SCC**	>70.0	58	Cisplatin	naïve, after C3	yes	6.9	22C3 CPS50	6 cm
pair 7*	31	IIIC	SCC	20.3	16,18	MK 3475-A18	naïve, after C2W1	yes	14.9	negative	6 cm
pair 13*	66	IIIC	SCC	25.7	68	MK 3475-A18	naïve, after C1	yes	11.7	unknown	6.6 cm
Good Prognosis group											
pair 17*	50	IIIB	SCC	39.1	unknown	Cisplatin	naïve, after C4	no	34.0	22C3 CPS15	4.5 cm
pair 19*	49	IIIC	SCC	16.7	unknown	Cisplatin	naïve, after C3	no	31.7	22C3 CPS3	6.5 cm
pair 20*	65	IIIC	SCC	6.5	other type	Cisplatin	naïve, after C3	no	30.3	22C3 CPS5	5.7 cm

* CCRT patients marked with an asterisk (*) in Table 2.

Pt : patients number

SCC, squamous cell carcinoma

MK 3475-A18: pembrolizumab 200 mg Q3weeks with weekly cisplatin 40 BSA

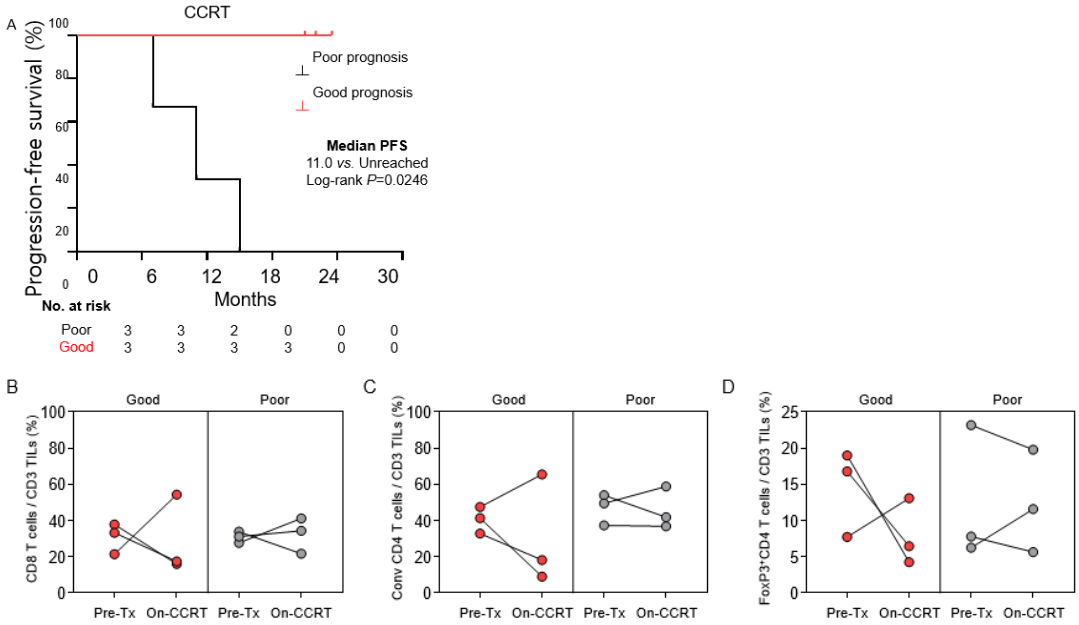

Figure 10. Differences in immunological and dynamic changes in TILs during CCRT based on prognosis

A) PFS classification of the good prognosis group and poor prognosis group

B, C, D) On comparing CD8 T cells, CD4 T cells, and Tregs in paired tissues, no differences based on prognosis are observed.

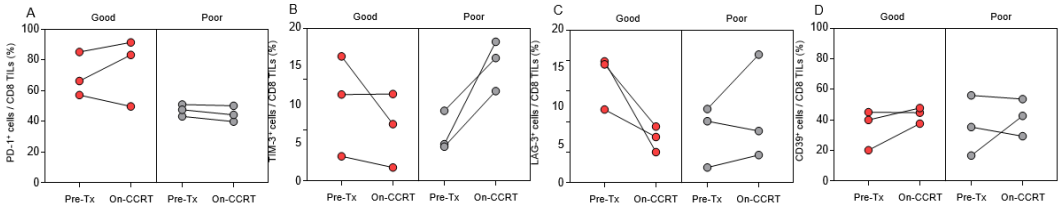

Figure 11. Differences in immunological changes in TILs during CCRT based on prognosis

A) No specific trends related to prognosis are observed for PD-1 expression.

B) TIM3 shows a tendency for a decrease in the good prognosis group.

C) LAG3 shows a tendency for a decrease in the good prognosis group.

D) There is no difference in CD39 expression based on prognosis.

4. DISCUSSION

Immunotherapy has recently emerged as the fourth major treatment modality for cancer, complementing chemotherapy, surgery, and radiation therapy. A notable example is the FDA approval in 2021 of the combination of chemotherapy with pembrolizumab for PD-L1-positive patients with recurrent, persistent, or metastatic cervical cancer. The phase 3 KEYNOTE-A18 study demonstrated a trend toward improved PFS in the group receiving CCRT with pembrolizumab compared to the group receiving CCRT with placebo. This suggests that immunotherapy may influence treatment outcomes by modulating the tumor microenvironment during treatment, highlighting the importance of understanding the tumor microenvironment for optimizing treatment strategies.

Studies on PBMCs and TILs have been conducted in various solid tumors. For example, research on ovarian and colorectal cancers has shown that TILs exhibit increased expression of cytotoxic T cells, accompanied by an increase in suppressive Tregs, compared to peripheral blood. In the present study, a comparison between PBMCs and TILs revealed an increased proportion of CD8 T cells and a marked upregulation of co-inhibitory receptors and exhaustion markers in TILs. These findings illustrate a fundamental characteristic of the tumor microenvironment, where lymphocytes become activated upon entering the tumor microenvironment to target tumor antigens. However, due to chronic antigen exposure, these lymphocytes eventually become dysfunctional and enter a state of exhaustion.

Cytotoxic chemotherapy depletes bone marrow cells, resulting in decreased production of various blood cells, including white blood cells, red blood cells, and platelets. Additionally, radiation therapy reduces T-cell counts in the treatment field. Therefore, it is inevitable that CCRT would lead to a reduction in CD45+ T cells in the tumor microenvironment. Similarly, a study on rectal cancer patients undergoing preoperative CCRT observed a decrease in total leukocyte count and lymphocyte count during the CCRT period, as measured by serial blood samples.

Granzyme B, an enzyme secreted by cytotoxic T cells and NK cells, induces apoptosis in target cells and plays a crucial role in attacking tumor cells in cancer patients. The increase in granzyme B

in CD8 TILs after treatment suggests treatment-induced activation of immune cells. The decrease in TCF-1 in CD8 TILs after CCRT reflects the process of T cells becoming dysfunctional due to chronic antigenic stimulation, a characteristic of exhausted T cells. This decrease also suggests a reduction in the function of memory T cells.

The decrease in the proliferative marker Ki-67 in TIL Tregs after CCRT suggests a decrease in the activation of immunosuppressive Tregs, indicating a shift toward enhanced immune responses.

Studies have shown that CCRT alters the tumor microenvironment, with one study demonstrating that radiotherapy alone or chemoradiotherapy increases PD-L1 expression and impacts the density of stromal CD8+TILs in patients with uterine cervical squamous cell carcinoma. Regarding PD-L1, this study had limited data, with only three patients having measurable PD-L1 levels in tumor cells before treatment, precluding an analysis of the effect of CCRT on PD-L1 expression in tumor cells. However, based on existing research, the observed increase in PD-L1 expression due to treatment can be interpreted as an enhancement of the tumor's immune evasion capabilities and adaptation to the therapy. This suggests that combining immune therapies such as anti-PD-L1 or anti-PD-1 antibodies can potentially enhance the effectiveness of CCRT.

The significant decrease in L1CAM expression in tumor cells can be interpreted in the context of previous studies on cervical cancer patients. These studies found that positive L1CAM expression (≥10% of tumor cells) was associated with shorter disease-free survival. Therefore, the reduction in L1CAM expression after CCRT may suggest a treatment-induced decrease in the aggressive characteristics of the tumor.

Although immunotherapies targeting PD-L1, PD-1, and CTLA-4 are actively being researched in various cancers, the need for further research into immune checkpoint inhibitors is emphasized due to drug resistance. Notable examples include TIM-3 and LAG-3. Studies on ovarian cancer have demonstrated that higher expression of TIM-3 is associated with advanced disease stages, highlighting the need for therapies such as anti-TIM-3 and anti-LAG-3. In the present study, the poor prognosis group exhibited increased expression of TIM-3 and LAG-3 after CCRT, suggesting the potential for combining therapies with anti-TIM-3 and anti-LAG-3 treatments.

A previous study on patients with cervical cancer found a significant increase in soluble TIM-3 levels during CCRT. In contrast, the present study found no significant changes in co-inhibitory receptor expression when comparing the entire on-treatment group. However, when patients were stratified by prognosis, the poor prognosis group exhibited a trend toward increased TIM-3 expression following CCRT.

In the prognosis-based group classification, the decrease in TIM-3 and LAG-expression 3 in the good prognosis group can be interpreted as a reduction in terminally exhausted T cells following CCRT, contributing to favorable outcomes. In contrast, the poor prognosis group exhibited worsening exhaustion despite treatment, leading to less favorable outcomes. Manifestation of $CD8^+$ T cell exhaustion before treatment or early in the course of treatment may suggest that immunotherapy can provide clinical benefits by enhancing the existing anti-tumor response of T cells. In contrast, $CD8^+$ T cell exhaustion observed at the end of treatment or after treatment indicates the persistence of T cell exhaustion despite treatment, suggesting a poor prognosis.

Regarding HPV infection, two patients tested negative for HPV. One patient, a 61-year-old woman with clear cell carcinoma stage Ia1, underwent radical hysterectomy and is currently in No Evidence of Disease (NED) status. The other patient, a 57-year-old woman with non-keratinizing squamous cell carcinoma stage Ib2 underwent radical hysterectomy followed by adjuvant RT and is also in NED status. Notably, both patients' HPV tests were performed on vaginal samples after hysterectomy, making it challenging to determine their initial HPV status.

Some limitations of this study should be acknowledged. The timing of sample collection after CCRT was not uniform. Additionally, the chemotherapy regimen during CCRT was not consistently cisplatin, with some patients receiving pembrolizumab. Furthermore, the number of patients and sample size for paired sample analysis were insufficient, which may limit the statistical power and generalizability of the findings.

5. CONCLUSION

The immune properties of TILs in cervical cancer appear to change dynamically during CCRT. The present study compared and analyzed the PBMCs and TILs of patients with LACC before treatment and observed the dynamic changes in the tumor microenvironment by assessing the differences in TILs before and after treatment. TILs, compared to PBMCs, exhibited a tumor microenvironment characterized by T cell exhaustion. Post-CCRT, there was a significant decrease in the number of immune cells. Notably, an increase in granzyme B expression and a decrease in TCF-1 expression were observed in CD8 TILs after CCRT. Additionally, a decrease in Ki-67 was observed in TIL Tregs. The changes in TIM-3 and LAG-3 expression before and after treatment varied depending on the treatment prognosis. These findings suggest that immunotherapy before CCRT may provide clinical benefits, particularly for the good prognosis group, where TIM-3 and LAG-3 expression decreases. Further studies are required to explore this potential therapeutic strategy.

REFERENCES

1. Sung H, Ferlay J, Siegel RL, Laversanne M, Soerjomataram I, Jemal A, et al. Global cancer statistics 2020: GLOBOCAN estimates of incidence and mortality worldwide for 36 cancers in 185 countries. CA Cancer J Clin. 2021:71:209–49.
2. The 2019 annual report of the Korean national cancer registration and statistics program
3. CDC United States Cancer Statistics: Data registries from 2013-2019
4. Eric PL, David SP T, Alexandra L, Mansoor R M, Takayuki E, Jitender T, et al. Comparison of global treatment guidelines for locally advanced cervical cancer to optimize best care practices: A systematic and scoping review. Gynecologic Oncology. 2022;167(2):360-372
5. Lalit K, Sudeep G. Integrating chemotherapy in the management of cervical cancer: a critical appraisal. Oncology. 2016;91(1):8-17
6. Akiko O, Takashi I, Yuki K, Shiho T, Kohsei T, Hiroshi N, et al. Tumor infiltrating lymphocytes predict survival outcomes in patients with cervical cancer treated with concurrent chemoradiotherapy. Gynecologic oncology. 2020;159(2):329-334
7. Patrícia R M, Christina M T M, Sarah A C, Adriana J O, Thayse B M, Larissa S C, et al. Cervical cancer patients that respond to chemoradiation therapy display an intense tumor infiltrating immune profile before treatment. Experimental and Molecular Pathology, 2019;111(104314)1-11
8. Yutuan W, Shuang Y, Shyamal G, Xuan P, Libing X, Xiaoming Z, et al. Clinical significance of peripheral blood and tumor tissue lymphocytes subsets in cervical cancer patients. BMC Cancer, 2020;20(173):1-12
9. Magdalena KB, Lana C, Jonna V, Christopher G T, Ryan M, Daniel H, et al. Detatiled characterization of tumor infiltrating lymphocytes in two distinct human solid malignancies show phenotypic similarities. Journal for ImmunoTherapy of Cancer, 2014;2(38):1-12

10. Andrew C, Karlo P, Christopher A K, Jedd D W. Clinical implications of T cell exhaustion for cancer immunotherapy. Nat Rev Clin Oncol. 2022;19(12):775-790
11. J M Herter, M Kiljan, S Kunze, M Reinscheid, O Ibruli, J Cai, et al. Influence of chemoradiation on the immune microenvironment of cervical cancer patients. Strahlenther Onkol, 2023;199(2):121-130.
12. Chao L, Xiaohui L, Aijie L, Wenxue Z, Rui H, Xiaoyu H, et al. Concurrent Chemoradiotherapy Increases the Levels of Soluble Immune Checkpoint Proteins in Patients with Locally Advanced Cervical Cancer. Journal of Immunology Research, 2022; 2022: 9621466.
13. Yasumasa M, Hiro S, Takuya K, Tiara B M P, Yuya Y, Kazutoshi M, et al. Analysis of radiotherapy-induced alteration of CD8+ T cells and PD-L1 expression in patients with uterine cervical squamous cell carcinoma. Oncol Lett. 2021;21(6):446.
14. Marlies S, Willem E C, Margit E V, Natalja T H, Enno J D, Jogchum J B, et al. L1 cell adhesion molecule(L1CAM) is a strong predictor for locoregional recurrences in cervical cancer. Oncotarget. 2017;8(50):87568-87581
15. Zhao-wei G, Ke D, Hui-zhong Z. The roles of CD73 in cancer. Biomed Res Int. 2014:2014:460654.
16. Rui L, Yuncong L, Rutie Y, Limei Y, Kemin L, Chuntang S, et al. The dynamic alteration of local and systemic tumor immune microenvironment during concurrent chemoradiotherapy of cervical cancer : A prospective clinical trial. International Journal of Radiation Oncology. 2021;110(5): 1432-1441
17. Hanqun Z, Shisheng T, Chunju F, Qi Z, Xue C, Yuncong L. PD-1/PD-L1 Correlates With the Efficacy of the Treatment of Concurrent Chemoradiotherapy in Cervical Cancer. Front Oncol. 2022 10:12:858164
18. Magdalena KB, Lana C, Jonna V, Christopher G T, Ryan M, Daniel H, et al. Detailed characterization of tumor infiltrating lymphocytes in two distinct human solid malignancies show phenotypic similarities. Journal for Immunotherapy of Cancer. 2014;2(38):1-12

19. Mateusz K, Dominika B, Aneta C P. The role of TIM-3 and LAG-3 in the microenvironment and immunotherapy of ovarian cancer. Biomedicines. 2022;10(11):2826
20. Michael J G, Marka R C. The paradox of radiation and T cells in tumors. Neoplasia 2022;31:1-16
21. Yongjoon L, Satbyol L, Sukkyung B, Yoondae H, Minsoo C, Hyuk H, et al. Temporal changes in immue cell composition and cytokines in response to chemoradiation in rectal cancer. 2018;8:1-10

ABSTRACT (IN KOREAN)

자궁경부암 치료 후 나타나는 종양 미세 환경의 면역학적 변화 및 예후에 따른 면역학적 변화의 차이에 대한 탐색

자궁경부암은 전 세계 여성에서 네 번째로 흔한 암이다. 국소 진행성 자궁경부암의 표준 치료는 시스플라틴 기반 동시 항암 방사선 치료로 이루어지지만, 5년 무병 생존율은 약 58%로, 생존률 향상을 위한 추가 연구가 지속적으로 필요하다. 다양한 암에서 CCRT 후 종양 침윤 림프구의 변화가 보고된 바 있으며, 종양 침윤 림프구에 대한 지속적인 연구는 기존 암 치료와 면역치료를 결합하는 새로운 통찰을 제공할 수 있다. 이 연구는 국소 진행성 자궁경부암 환자에서 치료 전 말초 혈액과 종양 침윤 림프구를 분석하여 기본적인 종양 미세 환경을 전반적으로 이해하고 동시 항암 화학 방사선 치료로 인한 종양 미세 환경의 변화를 예후에 따른 차이 분석을 포함하여 구체적으로 이해하고자 하였다.

2020년 3월부터 2023년 7월까지 총 41명의 대한민국 서울에 위치한 연세 암 병원 환자를 대상으로 하였다. 종양 침윤 림프구는 종양 조직(치료 전 샘플, n=39; CCRT 중 샘플, n=9)에서 분리하였고, 이것의 면역학적 특성은 다중 색상 유세포 분석을 통해 분석하였다. 혈액 샘플이 같이 있는 21명의 환자에 대해서는 말초혈액 단핵세포를 분리 후 유세포 분석을 하였다.

환자의 중간 연령은 51세였고, 국소 진행성 자궁경부암 환자는 36명(87.8%)이었으며, 가장 흔한 병기는 3C로 19명(46.3%)이 이에 해당했다. 2명의 환자를 제외하고는 모두 HPV 감염이 확인되었다.

동시 항암 화학 방사선 치료 중 $CD45^+$ 조혈세포가 유의미하게 감소하였으며, 전반적으로 종양 침윤 림프구는 말초 혈액 단핵 세포 보다 더 탈진된 상태를 보였다. CD8 종양 침윤 림프구에서 PD1, TIM3, LAG3, TIGIT을 포함한 억제성 수용체들은 치료 중 유의미한 변화를 보이지 않았으며, granzyme B 발현이 유의미하게 증가한 반면, $TCF1^+PD1^+CD8$ 종양 침윤 림프구(줄기세포 유사 CD8 T 세포)는 치료 중 유의미하게 감소하였다. 치료 중 증식성 Ki-67은 조절 T 세포에서 감소하였고, 종양 세포에서는 치료 후 $L1CAM^+$ 종양 세포가 유의미하게 감소하였다.

동시 항암 화학 방사선 치료 후 무진행 생존 기간을 18개월을 기준으로 환자를 분류한 결과, 치료 전 CD8 종양 침윤 림프구는 두 그룹 간에 차이가 없었다. CD8 종양 침윤 림프구에서 예후에 따른 $PD1^+$ 세포의 유의미한 차이는 발견할 수 없었지만, TIM3와 LAG3에 대한 분석에서는 좋은 예후 그룹에서는 TIM3와 LAG3의 발현이 감소하는 경향을, 나쁜 예후 그룹에서는 발현이 증가하는 경향을 확인했다. TIM3와

LAG3는 말기 탈진 상태의 T 세포에서 발현되므로, 이러한 세포의 감소는 더 나은 임상 결과와 연관될 수 있고, LAG3와 TIM3를 표적하는 면역 치료를 조합하는 것에 대한 고찰을 해볼 수 있다.

종양 침윤 림프구들의 면역학적 특성은 자궁경부암에서 동시 항암 화학 치료 중 동적으로 변화하는 것으로 보인다. 자궁경부암의 치료 전과 치료 중 종양 미세 환경의 변화를 분석하고, 예후에 따른 차이를 이해하는 것은 기존 치료와 면역치료를 결합하는 새로운 전략을 제시하는 데 도움이 될 수 있다.

핵심되는 말: 자궁경부암, 동시 항암 화학 방사선 치료, 종양 침윤 림프구, 종양 미세 환경